JOURNAL OF OPTOELECTRONICS AND ADVANCED MATERIALS Vol. 10, No. 8, August 2008, p. 2047 - 2051

Varieties of carbon nanostructures obtained by the AC arc discharge method

G. RUXANDA[a*], M. STANCU[a], S. VIZIREANU[b], G. DINESCU[b], D. CIUPARU[a]
[a]*Petroleum Gas University of Ploiesti, Physics Department, Bucharest Blvd. 39, 100680 Ploiesti, Romania*
[b]*National Institute for Laser, Plasma and Radiation Physics, Magurele MG 36, 077125, Bucharest, Romania*

Here we report on the varieties of carbon nanostructures obtained in an AC arc discharge with graphite electrodes loaded with Ni and Fe powders. The nanostructures produced were characterized by TEM and Raman spectroscopy. Because there is a lack of agreement concerning the active regions for the formation of carbon nanostructure with respect to the arc position in the reaction chamber, we have sampled and characterized the nanostructures formed in different regions in our arc discharge reactor. The Raman spectra indicate the presence of the "crystalline" phases in the material. The TEM results confirm that MWCNT (multi walls carbon nanotubes) are dominant, but also single wall nanohorns, polyhedral nanostructures, onion like graphite particles can be found in the plasmogenic product collected from different regions of the arc chamber.

(Received March 1, 2008; accepted June 30, 2008)

Keywords: Arc discharge, Carbon nanostructures,TEM investigation.

1. Introduction

For the synthesis of carbon nanostructures different techniques were used such as: laser vaporization [1,2], electric arc discharge [3-5], chemical vapor deposition (CVD) [6-8], pyrolysis of hydrocarbons [9-11] and combined methods. By using an electric arc discharge with two graphite electrodes, Iijima discovered in 1991 cylindrical nanostructures named „multiwall carbon nanotubes" (MWNCT) [12]. The electric arc discharge method, either in direct current or in the alternating current, "DC arc discharge", "AC arc discharge", became one of the most widespread and efficient route among the carbon nanostructures synthesis techniques. The difference between the two synthesis options (DC and AC) was evidenced in part by Huang Zeng and co-workers [13]. Although the application of the AC arc discharge technique, also known as the "violent method" [14], has limitations and leads to the formation of heterogeneous plasmogenic products, there are still many technical venues to improve the selectivity. Handling of the large number of parameters of the electric arc chamber (nature of the gas used, pressure, the current of discharge, distance between electrodes, the metal or metal catalysts mixture, the purity of electrodes, etc) allows optimization of this technique and improvement of its selectivity.

It is well known that a large part of the energy of the electric arc occurs in thermal radiation [15] and not only the plasma composition, but also the substrate temperature strongly influences the morphology of the grown material. Depending on the reflectivity and the geometry of the chamber of the electric arc, this energy can be transferred to the wall, returned to the volume of the electric arc, heating the gas, so different temperature values and plasma compositions can be found in different reactor regions. In this work we study and describe the varieties of carbon nanostructures obtained at different locations in the chamber of the AC electric arc with graphite electrodes, by using Raman and TEM investigation of the produced samples.

2. Experimental

2.1. Experimental setup

The reactor is designed in such a way that allows the creation of a buffer gas flow (argon) in close proximity of the electric arc volume aiming to quickly remove the active nanostructure "seeds" formed by the direct influence of the thermal radiation emitted by the electric arc.

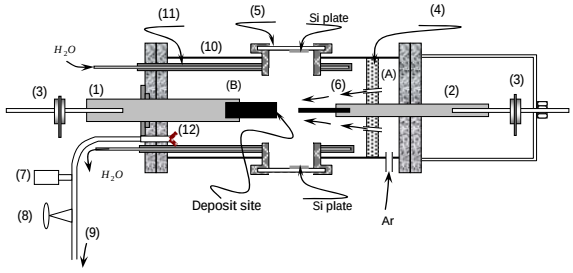

Fig. 1. Set-up diagram: (1) Fixed holder for the thick carbon electrode; (2) Movable holder for the thin carbon rod; (3) electric contact to the AC power supply; (4) separating wall; (5) optical window; (6) flow inlet for the Ar buffer gas; (7) pressure gauge; (8) vacuum valve, (9) vacuum pump; (10) reactor wall; (11) cooper made cylindrical cooler; (12) trap

The sketch of the setup used for obtaining the plasmogenic product containing carbon nanostructures is displayed in Figure 1. It consists of a stainless steel discharge chamber, provided with windows for process

visualization and limited at both ends with flanges which allow the gas and electrical feeding through. The separating wall (skimmer, 4) splits the main body of the vacuum chamber in two parts: the pressure chamber (A) and the chamber of the electric arc (B). The argon gas passes from chamber (A) in chamber (B) through the skimmer wall provided with 12 nozzles. Their openings are oriented by design towards the zone where the electric arc is formed and create a flow of Ar enriched gas in the close proximity of the electric arc. A cylindrical cooler (11) is placed coaxially to the electrodes. It has two large slots, with the openings directed to the optical windows. On the optical windows (5) Si wafers are attached for collecting the possible plasmogenic product resulting from the experiment. The Si plates are located at 112 mm from the centre of the electric arc. Other part of the plasmogenic product resulting is deposited on the internal wall of the cooler, on the thick and the thin electrodes, which takes a fraction of the heat generated by the electric arc.

2.2 Electrodes and their preparation

We used in our experiments graphite electrodes of unequal diameters, with ash content of below 2 ppm. The diameter of the thin electrode is 3.05 mm and its effective length is 105 mm. The diameter of the thick electrode is 12.05 mm and its effective length is 50 mm. The thin electrode was drilled for 17 mm along its longitudinal axis in the centre of its circular section, making a channel of 1.3 mm diameter. The channel was filled with a mixture of metallic powder and graphite. We used mixtures of Fe and graphite (95% C and 5% Fe) and of Ni and graphite (95% C and 5% Ni).

2.3 Collection of samples

Apparently, the plasmogenic product is scattered all over the inner surfaces of the reactor. During our experiments we did not observe any consumption of the thick electrode; on the contrary, a cone shaped deposit formed at the end of the thick electrode in contact with the plasma. After each experiment the following types of samples were selected:

a) Samples formed on the Si wafers fixed on the optical windows (5) noted $\mathbf{P}_{(Fe\text{-}Si)}$, $\mathbf{P}_{(Ni\text{-}Si)}$. Those deposits are directly exposed to the thermal radiation emitted by the electric arc and represent less than 0.001% of the mass consumed from the thin electrode. The energy dissipated from the electric arc by thermal radiation represents almost half of the energy emitted by the electric arc [15]. The high intensity of the thermal radiation incident on the Si plates could influence the formation of carbon nanostructures depending on the metal used as catalyst.

b) Samples collected from the deposit formed on the thick electrode, noted $\mathbf{P}_{(Dep\text{-}Fe)}$, $\mathbf{P}_{(Dep\text{-}Ni)}$. During the experiment, the deposit formed on the thick electrode is under the direct impact of the species from the plasma of the electric arc. This deposit, with a solid spongy aspect, is easily removed from the thick electrode by cleavage upon plans perpendicular to the arc axis.

c) During the experiment, the temperature of the thin electrode is very high, almost $T_1 \approx 2700$ K. After experiments, the lateral surface of the thin electrode has a rough aspect. The rough layer was removed from the thin electrode by sonication the remaining piece in ethanol. The samples from this deposit were noted $\mathbf{P}_{(Es\text{-}Fe)}$, $\mathbf{P}_{(Es\text{-}Ni)}$. The deposit formed on the remaining thin electrode is not under direct influence of the thermal radiation, neither under the influence of the species from the plasma of the electric arc.

3. Results and discussion

In arc discharge methods typically five products are obtained [16]: amorphous carbon, fullerenes, graphite nanoparticles (“graphite polyhedral crystals” [17] or polyhedral graphitic nanoparticles [18]), metallic particles enveloped by graphite layers (when a catalyst is used) and many types of CNTs. We have searched our samples for the presence of the crystalline forms of carbon listed above by Raman spectroscopy and TEM investigations.

3.1 Raman investigations

The Raman spectroscopy was performed with the Raman Spectrometer NRS-3000 Series equiped with two internal lasers, 532 nm ($E_L = 2.33$ eV) and 785 nm (1.49 eV), having a beam diameter with a minim of 1 μm.

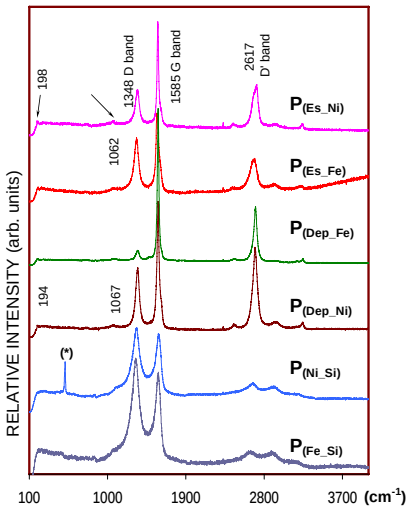

Fig. 2. Raman spectra of samples collected from different region of arc

In is well known that the Raman spectra give information about the presence of ordered phases in carbonic materials [19-23]. These phases are signalled by the presence of the so-named G-band at around 1580 cm^{-1}.

We can observe this G peak for all the samples. Besides, the D band around 1335 cm^{-1} and the second order of the G and D bands are observed. The G band is related to the in-plane vibration of graphitic structures

with sp^2 type of bond and the D peak is assigned to disordered or defective structures of the material. The presence of the second order of Raman spectra is an additional proof of the high order degree of the samples. Another possible band characteristic to the radial breathing mode of single wall nanotubes, which should appear in the 100-500 cm^{-1} region, does not appear or is too low to extract any information on these nanostructures [23].

The intensity ratio of the D-band to the G-band $R = I_D/I_G$ is considered a measure of the quality of carbon nanostructures [21-22]. For the investigated samples the following values were found: $R_{P(Ni\_Si)}$= 1.159, $R_{P(Fe\_Si)}$= 1.072, $R_{P(Dep\_Fe)}$= 0.369, $R_{P(Dep\_Ni)}$=0.631, $R_{P(Es\text{-}Ni)}$= 0.605, $R_{P(Es\text{-}Fe)}$= 0.675. From these values we conclude that the material collected from the thick electrode ($P_{(Dep\_Fe)}$, with the lower R value) is the best in the experiment with respect to the presence of the ordered phases. The material with disordered and defective structures was obtained in the deposits from the outside zone of the arc, onto the silicon wafer (bottom traces in Figure 2).

From the shape and intensity distribution of the bands in the Raman spectra we expect to find various graphitic structures in the deposits, such as glassy carbon and carbon nanotubes. A detailed view of the nanostructures suggested by the Raman investigation is presented below, as obtained from TEM measurements.

3.2 TEM investigations

The TEM investigations were performed using a TECNAI/FEI F20 instrument equipped with a 200 kV electron gun.

Selected TEM images of the material deposited on the Si substrates (samples $P_{(Fe\text{-}Si)}$, $P_{(Ni\text{-}Si)}$) are presented in Figures 3 and 4. These images show the presence of MWCNTs. The interplanar spacing between consecutive walls determined from the circled zones in Figure 3 is 0.38 nm, which corresponds to curved graphite assemblies.

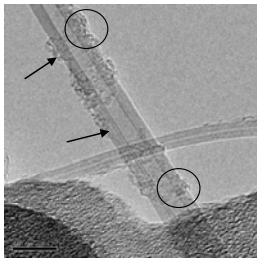

*Fig. 3. Image of the material extracted from the deposit on Si substrate (**$P_{(Fe\text{-}Si)}$**, experiments with mixture Fe+C)*

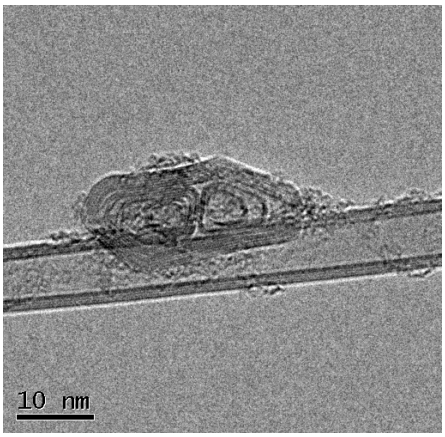

a)

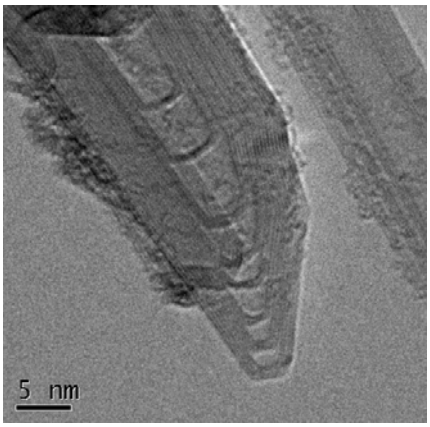

b)

*Fig. 4. **a)** MWCNT with an attached crystalline particle; b) MWCNT with pinnacle cap ended by pairs of graphene sheets (sample type $P_{(Ni\text{-}Si)}$)*

a) The nanotubes in Figure 3 have external diameters of 3.5 nm and respectively 8.0 nm and the inner diameters are 1.0 and 3.1 nm, respectively. There are graphitic particles frequently stuck on their external wall (small circle in Figure 3) apparently not bonded to the MWCNT (see Figure 4a). Other defects observed are uneven spacing of graphitic layers in the wall, as shown in the region indicated with arrows in Figure 3. Many of the MWCNTs have end caps which are closed in steps by pairs of graphene sheets (pinnacle tip capped, Figure 4b).

This behaviour, i.e. pair wall closing structures, was observed in multiwall nanotubes with a large number of walls. Similar TEM images were previously reported [16], but for materials deposited by DC arc discharge.

b) The samples collected from the thick electrode (Figures 5 a, b, c, d) show characteristics similar to those collected from the silicon wafer. MWCNTs with symmetric caps are also observed (Figure 5c). Moreover, in this deposit polyhedral carbon forms with buckled faces have been identified (Figure 5 d).

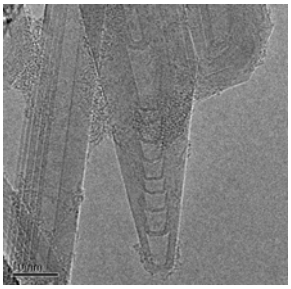

a

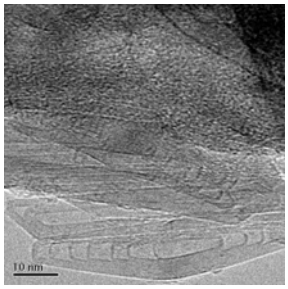

b

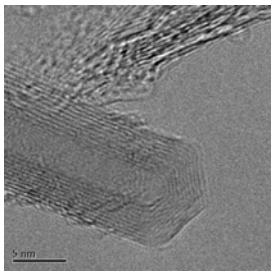

c

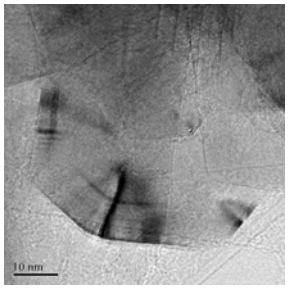

d

Fig. 5. *TEM images of the material collected from the thick electrode: a) pinnacle capped end (a and b), symmetric cap (c), polyhedral (d) form ($P_{(Dep-Ni)}$ and $P_{(Dep-Fe)}$) .*

c) Figure 6 reveals details of the material obtained by sonication of the thin electrode. As in the previous cases, MWCNT are frequently present. The image of an MWCNT with an external diameter of about 5 nm and inner diameter of 0.7 nm is shown in Figure 6a. Besides, peculiar shapes are identified in this region. Bended carbon ribbons, specific to glassy carbon are shown in Figure 6b. In Figure 6c randomly distributed open structures are presented, consisting of graphene sheets, which can be assigned to the family of nanohorns or to open fullerene shells [24-26]. In Figure 7d an onion like structure is presented, superimposed over polyhedral crystalline carbon particles.

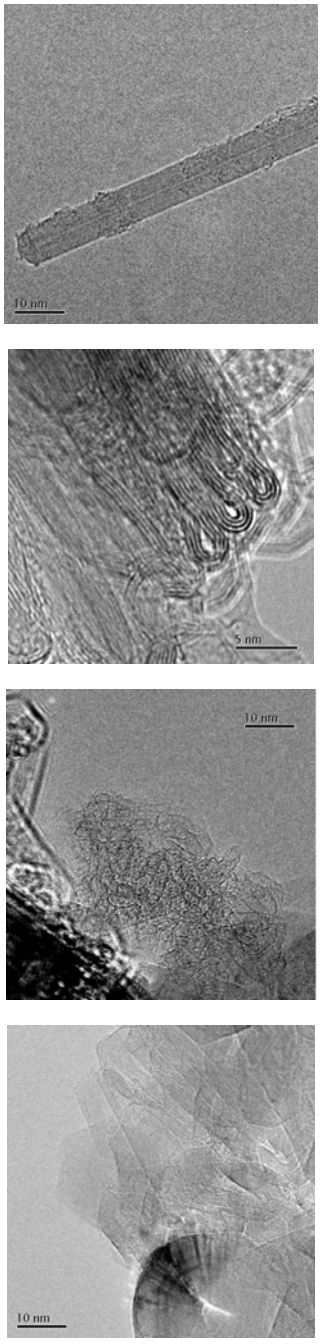

Fig. 6. TEM images of the material collected from the thin electrode ($P_{(Es-Fe)}$ and $P_{(Es-Ni)}$): MWNT (a), curved graphite ribbons (b), open single wall structures (c), carbon onion (d).

4. Conclusions

Experiments of synthesis of carbon nanostructures in an argon AC arc discharge with graphite electrodes of different diameters loaded with Ni and Fe powders are presented. During the arc discharge operation the thin electrode is consumed, nanostructured carbonic material is deposited all over the reaction chamber and a deposit is formed at the end of the thick electrode facing the electric arc. Samples were collected from the silicon wafers positioned far from the arc, from the deposit on the thick electrode and from the external surface of the thin electrode. All samples showed the presence of a large variety of multilayer nanostructures like MWCNT, deformed MWCNT, polyhedral graphitic nanoparticles. The Raman investigations indicate the surface of the thin electrode (not exposed directly to the arc radiation, but having the highest temperature) as being the most suitable for obtaining ordered graphitic structures. In particular, the TEM investigations revealed the presence in this region of special graphitic forms like open single wall nanostructures, ribbons and onions.

Acknowledgments

The financial support from the Romanian Ministry of Education and Research received in the frame of CEEX and PNCDI II Research Programmes is highly acknowledged. We kindly acknowledge the useful discussions with Dr. Leona Nistor from the National Institute for Material Research Magurele, Bucharest, Romania

References

[1] H. Dai, A. G. Rinzler, P. Nikolaev, A. Thess, D. T. Colbert, R. E. Smalley, Chem. Phys. Lett., **260**, 471. (1996).

[2] T. Guo, P. Nikolaev, A. Thess, D. T. Colbert, R. E. Smalley, Chem. Phys. Lett., **249**, 49, (1995).

[3] T. W. Ebbesen, Nature **358**, 220 (1992).

[4] M. Tomita, Y. Saito, T. Hayashi, Jap. J. Appl. Phys. **32**, L280, (1993).

[5] D. S. Bethune, C. H. Kiang, M. S. Vries, G. Gorman, R. Savoy, J. Vasquez, Nature **363**, 605. (1993)

[6] S. Fan, M. G. Chapline, N. R. Franklin, T. W. Tombler, A. M. Cassell, H. Dai, Science **283**, 512, (1999).

[7] Q. H. Wang, A. A. Seltlur, J. M. Lauerhaas, J. Y. Dai, E. W. Seelig, R. P. H. Chang Appl. Phys. Lett. **72**, 2912. (1998).

[8] X. Xu, G. R. Brandes, Appl. Phys. Lett. **74**, 2549. (1999).

[9] W. K. Hsu, J. P. Hare, M. Terrones, H. W. Kroto, D. R. M. Walton, P. J. F. Harris, Nature **377**, 687 (1995).

[10] W. K. Hsu, J. P. Hare, M. Terrones, H. W. Kroto, D. R. M. Walton, Chem. Phys. Lett. **262**, 161 (1996).

[11] H. M. Cheng, F. Li, G. Su, H. Y. Pan, L. L. He, X. Sun, M. S. Dresselhaus, Appl. Phys. Lett. **72**, 3282 (1998).

[12] S. Iijima, "Helical microtubules of graphitic carbon", Nature, vol. 354, Nov. 1991, p. 56-58.

[13] Huang Zeng, Ling Zhu, Guangming Hao, Rongsheng Sheng, Carbon, **36**(3), 259 (1998).

[14] Thomas Laude, Boron Nitride Nanotubes Grown by non-ablative Laser heating: Synthesis, Characterisation and Growth Processes, Presented on February, University of Tsukuba, Japan, (2001)

[15] E. G. Gamaly, T. W. Ebbesen, Phys. Rev., B, Vol. 52, no. 3, 15 July (1995).

[16] D. N. Borisenko, N. N. Kolesnikov, M. P. Kulakov V. V. Kveder, International Journal of Nanoscience, **1**, (3&4), 235 (2002).

[17] P. T. Heng, S, Dimovski Yury Gogotsi Y, Phil. Trans. R. Soc. Lond. A, **362**, 2289 (2004).

[18] J-F. Colomer, P. Piedigrosso, I. Willems, C. Journet, P. Bernier, G. Van Tendeloo, A. Fonseca, B. Nagya J., J. Chem. Soc., Faraday Trans., **94**, 3753 (1998).

[19] M. Chhowalla, K. B. K. Teo, C. Ducati, N. L. Rupesinghe, G. A. J. Amaratunga, A. C. Ferrari, D. Roy, J. Robertson, W. I. Milne, J. Appl. Phys **90**, 5308, (2001)

[20] Z. H. Ni, H. M. Fan, Y. P. Feng, Z. X. Shen, B. J. Yang, Y. H. Wu, J. Chem. Phys., **124**, 204703. (2006)

[21] S. Kurita, A. Yoshimura, H. Kawamoto, T. Uchida, K. Kojima, M. Tachibana, P. Molina-Morales, H. Nakai, J. Appl. Phys., 97, 104320, (2005)

[22] J. Kastner, T. Pichler, H. Kuzmany, S. Curran, W. Blau, D. N. Weldon, M. Delamesiere, S. Draper, H. Zandbergen, Chem. Phys. Lett. **221**, 53. (1994)

[23] M.S. Dresselhaus, G. Dresselhaus, R. Saito, A. Jorio, Physics Reports **409**, 47 (2005)

[24] Mirabile Gattia D., Vittori Antisari M., Marazzi R., Nanotechnology 18, 255604, (2007).

[25] Zhang M., Yudasaka M., Miyawaki J., Fan J., Iijima S., J. Phys. Chem. B, September 22, (2005).

[26] Bekyarova E., Murata K., Yudasaka M., Kasuya D., Iijima S., Tanaka H., Kahoh H., Kaneko K., The Journal Of Physical Chemitry, Volume 107, Number 20, May 22, (2003)

*Corresponding author: adnaxur@yahoo.com